Surface Functionalization of Cadmium Sulfide Quantum-Confined Nanoclusters. 5. Evidence of Facile Surface-Core Electronic Communication in the Photodecomposition Mechanism of Functionalized Quantum Dots†

Jonathan G. C. Veinot, Josie Galloro, Linda Pugliese, Robert Pestrin, and William J. Pietro*

Department of Chemistry, York University, 4700 Keele Street, Toronto, Ontario, Canada M3J 1P3

Received July 21, 1998. Revised Manuscript Received November 5, 1998

The photoinduced decomposition of dimethylformamide suspensions of 10 different surface-substituted thiolate-capped 30 Å cadmium sulfide quantum-confined nanoclusters was studied. HPLC analysis demonstrates that decomposition proceeds at a constant rate and produces only precipitated cluster aggregates and the symmetric disulfide corresponding to the thiolate cap as the only organic product. The dependence of the disulfide photogeneration kinetics on the Hammett σ_p parameter for the remote substituent indicates that both electron donors and acceptors enhance the rate and is mimicked by nanocluster fluorescence quenching efficiencies of the substituents, suggesting a photodecomposition mechanism involving facile electronic communication between the quantum dot core and the remote substituent. Further evidence for the mechanism was obtained from the product distribution ratios of the photodecomposition of a 4-nitrothiolate/4-methylthiolate-mixed surface nanocluster.

Introduction

Q-size metal or semiconductor nanoclusters, more commonly known as quantum-confined nanoclusters or quantum dots, are currently the focus of much intensive investigation as these interesting new materials hold the potential for revolutionary impact on the electronics industry.[1] Quantum dots are formed when the particle size of a metal or semiconductor falls below the Bohr radius of the material's exciton, but remains large enough to impart band structure.[2] This size domain is typically between ten and a few hundred angstroms in diameter, although particles as large as a tenth of a micron have been loosely referred to as quantum dots. Quantum-confined nanoclusters possess optical and electronic properties quite different from their bulk counterparts, primarily due to the so-called quantum confinement effect, which arises from a shift in the wave mechanics of the conduction electrons from a Bloch function to that of a particle-in-a-sphere. New materials based on quantum-confined nanoclusters may give rise to the fabrication of electronic devices possessing properties heretofore unheard of in conventional semiconductor electronics, such as dynamically tunable light-emitting diodes, tunnel and negative resistance devices, unusual nonlinear optical materials, and Coulomb blockade devices such as single-electron diodes and transistors.[3]

The fabrication of such electronic devices will likely be predicated on the covalent attachment of molecular moieties such as quantum wires, electroactive fragments, chromophores, luminophores, and soforth, to the nanocluster surface. We have been investigating the chemical activation and reactivity of the surface of cadmium sulfide nanoclusters prepared by the well-known kinetic trapping method.[4,5] This method provides nanoclusters of surprisingly good monodispersity, which are conveniently enveloped in a shell of organic aromatic "capping" molecules. Our strategy has been to use these caps as an entry point into surface functionalization. We have recently demonstrated that CdS nanoclusters can be surface-activated, and subsequently bound covalently to a wide variety of interesting chemical moieties without disruption of the semiconductor core.[6]

* To whom correspondence should be addressed.

† For part 4 in this series, see ref 6d.

(1) For recent reviews see: (a) Alivisatos, A. P. *J. Phys. Chem.* **1996**, *100*, 13266. (b) Weller H. *Angew. Chem., Int. Ed. Engl.* **1993**, *32*, 41. (c) Schmid, G. *Chem. Rev.* **1992**, *92*, 1709. (d) Steigerwald, M. L.; Brus, L. E. *Acc. Chem. Res.* **1990**, *23*, 183. (e) Henglein, A. *Chem. Rev.* **1989**, *89*, 1861.

(2) (a) Merkt, U.; Sikorski, Ch. *Semiconduct. Sci. Technol.* **1990**, *5*, 182. (b) Fulton, T. A. *Nature* **1988**, *346*, 408. (c) Zorman, B.; Ramakrishna, M. V.; Friesner, R. A. *J. Phys. Chem.* **1995**, *99*, 7649.

(3) (a) Klein, D. L.; Roth, R.; Lim, A. K. L.; Alivisatos, A. P.; McEven, P. L. *Nature* **1997**, *389*, 699. (b) Moskovits, M., personal communication, 1997. (c) Moskovits, M.; Xu, J. M., U.S. Patent 5,581,091, 1996.

(4) Herron, N.; Wang, Y.; Eckert, H. *J. Am. Chem. Soc.* **1990**, *112*, 1322.

(5) Krishnamurthy, S.; Aimino, D. *J. Org. Chem.* **1989**, *54*, 4458.

(6) (a) Noglik, H.; Pietro, W. J. *Chem. Mater.* **1994**, *6*, 1593. (b) Noglik, H.; Pietro, W. J. *Chem. Mater.* **1995**, *7*, 1333. (c) Veinot, J. G. C.; Ginzburg, M.; Pietro, W. J. *Chem. Mater.* **1997**, *9*, 2117. (d) Veinot, J. G. C.; Galloro, J.; Pugliese, L.; Bell, V.; Pestrin, R.; Pietro, W. J. *Can. J. Chem.* (Special Issue on Materials Science) to be published in Nov 1998.

10.1021/cm980513t CCC: $18.00
Published on Web 02/25/1999

In this contribution we address the question of electronic communication between the semiconductor core and a remote surface substituent covalently bound to the nanocluster, a necessary criterion for the eventual realization of nanocluster-based electronic devices.

Experimental Section

Chemicals. All solvents were obtained from Caledon Laboratories. Reagent grade dimethylformamide (DMF) and acetonitrile were dried over 4 Å molecular seives and filtered prior to use. Methanol (HPLC grade), diethyl ether, and acetic acid were used as received. Water was purified first by passage through a Sybron-Barnstead D8902 mixed-bed ion-exchange column and then freed from organic impurities using a Sybron-Barnstead D8204 activated charcoal filter. Water used for HPLC analyses was subsequently filtered through a Millipore 0.2 μm membrane. All deuterated solvents used for NMR analysis were purchased in sealed ampules from Cambridge Isotope Laboratories (Andover, MA) and used immediately upon opening. Cadmium acetate dihydrate (Aldrich reagent grade) was recrystallized (and concurrently dehydrated) from glacial acetic acid and dried in vacuo for 24 h at 100 °C. All commercially available thiols were obtained from Aldrich and purified as follows. 4-Mercaptophenol was distilled at reduced pressure, 4-mercaptoaniline was sublimed at 60 °C and 100 mTorr, and 4-nitrothiophenol, 4-mercaptotoluene, and 4-chlorothiophenol were recrystallized from absolute ethanol. After purification all thiols were stored under dry N_2 at temperatures below 18 °C. *p*-Hydroxybenzonitrile, *N*,*N*-dimethylthiocarbamoyl chloride, 1,4-diazobicyclo[2.2.2]octane (DABCO), phenyl disulfide, 4,4′-hydroxyphenyl disulfide, 4,4′-aminophenyl disulfide, sodium sulfide nonahydrate, and dicyclohexylcarbodiimide (DCC) were purchased reagent grade from Aldrich and used as received. Thionyl chloride was obtained from BDH and vacuum-distilled immediately prior to use.

Mercaptan Synthesis. *4-Cyanothiophenol (**1**).* 4-cyanothiophenol was prepared using the procedure outlined by Aimino and co-workers.[5] Following recrystallization from absolute ethanol, the yellow solid was characterized using mp 46−48 °C. ^{1}H NMR (DMSO-d_6) δ (ppm): 7.74 (d, 2H, C3−H), 7.55 (d, 2H, C2−H), 6.26 (br s, 1H, SH). EI-MS (*m*/*z*): 135, 108, 91, 84, 69, 63, 45, 28.

*4-Carboxythiophenol (**2**).* Two grams (14.8 mmol) of (**1**) were dissolved in 40 mL of a 2.5 M methanolic sodium hydroxide solution and refluxed for 28 h in a nitrogen atmosphere. The resultant solution was acidified to pH 2 with 6 M HCl. The resulting yellow solid was recrystallized from absolute ethanol and characterized using mp 215−218 °C (lit. 219 °C). ^{1}H NMR (DMSO-d_6) δ (ppm): 12.9 (br s, 1H, acid H), 7.84 (d, 2H, C3−H), 7.44 (d, 2H, C2−H), 5.92 (br s, 1H, SH). EI-MS (*m*/*z*): 154, 137, 109, 65, 39, 28.

Nanocluster Preparation. All CdS nanoclusters were prepared by modifications of the kinetic trapping method of Herron et al.[4] All solutions used for the preparation of CdS nanoclusters were thoroughly degassed with dry N_2, and all procedures were performed in an inert atmosphere under subdued light.

*Phenolic (**3b**, QDOH) and Aniline (**3c**, QDNH$_2$) CdS Nanoclusters, and Their Esterified (**3j**) and Amidized (**3k**) Derivatives.* Phenolic and aniline surface CdS nanoclusters and corresponding esterified and amidized derivatives were prepared as previously described.[6c,d]

*4-Chlorobenzene Surface CdS Nanoclusters (**3d**).* Sixty-five milliliters of a solution containing 0.61 g (2.6 mmol) of cadmium acetate in 1:1:2 CH_3OH:CH_3CN:H_2O (v:v:v) was rapidly mixed with 65 mL of a solution containing 0.3 g (1.4 mmol) of $Na_2S{\cdot}9H_2O$ and 0.8 g (5.5 mmol) of 4-chlorothiophenol in the same solvent system, and the mixture was stirred rapidly, yielding an immediate yellow precipitate. The reaction mixture was stirred at room temperature for 12 h and then concentrated to half its original volume. The resultant yellow precipitate was isolated by centrifugation and subsequently washed by successive sonication/centrifugation cycles in, sequentially, water, methanol, acetone, and diethyl ether. The solid was dried in an evacuated drying pistol for 12 h at 80 °C over KOH. Yield: 0.4 g. ^{1}H NMR (DMSO-d_6) δ (ppm): 6.7−7.2 (m, 4H, arom). FT-IR (KBr), ν (cm^{-1}): 3070 (w, arom C−H str), 1880, 1730 (w, 1,4-disub ϕ ovrtn), 1613 (m), 1570 (m), 1470 (s, ring C═C), 1425 (m), 1385 (s), 1089 (s, ϕ-Cl str), 1009 (m, ϕ-S), 811 (m, ϕ C−H out-of-plane bend), 540 (m), 488 (m). UV−vis (DMF) λ_{max} (nm): 310 (edge), 360 (shldr).

*4-Nitrobenzene Surface CdS Nanoclusters (**3e**).* Seventy-five milliliters of a solution containing 2.5 g (11 mmol) in 1:1:2 CH_3OH:CH_3CN:H_2O (v:v:v) was rapidly mixed with 75 mL of a solution containing 1.25 g (5.8 mmol) of $Na_2S{\cdot}9H_2O$ and 2.5 g (16 mmol) of 4-nitrothiophenol in the same solvent system, and stirred for 16 h. The resulting orange precipitate was repeatedly washed by successive sonication/centrifugation cycles in, sequentially, water, acetone, and diethyl ether, and dried at 65 °C in vacuo overnight. Yield: 1.16 g. ^{1}H NMR (DMSO-d_6) δ (ppm): 7.4−8.3 (m, 4H, arom). FT-IR (KBr) ν (cm^{-1}): 3094 (w, arom C−H str), 1920, 1750 (w, 1,4-disub ϕ ovrtn), 1613 (m), 1573 (m), 1509 (vs, NO_2 assym str), 1474 (s, ring C═C), 1339 (vs, NO_2 sym str), 1107 (m), 1088 (s), 1009 (m, ϕ-S), 853 (m), 738 (m, ϕ C−H out-of-plane bend), 680 (m), 531 (m), 467 (m). UV−vis (DMF) λ_{max} (nm): 324, 400, 502.

*4-Methylbenzene Surface CdS Nanoclusters (**3f**).* One hundred fifty milliliters of a solution containing 5.0 g (22 mmol) of cadmium acetate in 1:1:2 CH_3OH:CH_3CN:H_2O (v:v:v) was rapidly mixed with 150 mL of a solution containing 2.5 g (11 mmol) of $Na_2S{\cdot}9H_2O$ and 4.8 g (38 mmol) of 4-mercaptotoluene in the same solvent system, and stirred for 16 h. The resulting precipitate was washed by successive sonication/centrifugation cycles with, sequentially, water, acetonitrile, acetone, and diethyl ether and then dried overnight in vacuo at 65 °C. Yield: 1.3 g. ^{1}H NMR (DMSO-d_6) δ (ppm): 6.7−7.2 (m, 4H, arom). FT-IR (KBr) ν (cm^{-1}): 3013 (m, arom C−H str), 2970 (w), 2916 (w), 2860 (m, aliph C−H str), 1887 (w, 1,4-disub ϕ ovrtn), 1488 (s, ring C═C), 1445 (m), 1395 (m), 1375 (w), 1299 (w), 1208 (w), 1085 (s), 1014 (s, ϕ-S), 798 (m, ϕ C−H out-of-plane bend), 624 (w), 487 (m). UV−vis (DMF) λ_{max} (nm): 310 (edge), 390 (shldr).

*4-Cyanobenzene Surface CdS Nanoclusters (**3g**).* Fifteen milliliters of a solution containing 0.48 g (2.1 mmol) of cadmium acetate in 1:1:2 CH_3OH: CH_3CN:H_2O (v:v:v) was rapidly mixed with 15 mL of a solution containing 500 mg (3.7 mmol) of 4-cyanothiophenol and 0.24 g (1 mmol) of sodium sulfide nonahydrate in the same solvent mixture. The reaction mixture was stirred in subdued light and a nitrogen atmosphere for 12 h and yielded a yellow/white precipitate. The precipitate was isolated using conventional centrifugation and washed repeatedly using sonication/centrifugation cycles in water, methanol and diethyl ether. The solid was dried in an evacuated drying pistol for 12 h at 80 °C over KOH. Yield 0.31 g. ^{1}H NMR (DMSO-d_6) δ (ppm): 7.2−8.0 (m, 4H arom); FT-IR (KBr) ν (cm^{-1}) 3044 (w, arom C−H str), 2243 (s, CN str), 2221 (s), 1582 (s), 1476 (s, C═C), 1177 (w), 1082 (s), 1011 (m, ϕ-S), 817 (m, ϕ C−H out-of-plane bend), 584 (w), 542(m). UV−vis λ_{max} (DMF) (nm): 320(edge), 395 (shldr).

*4-Carboxybenzene Surface CdS Nanocluster (**3h**).* Five milliliters of a solution containing 0.09 g (0.39 mmol) of cadmium acetate in 1:1:2 CH_3OH:CH_3CN:H_2O (v:v:v) was rapidly mixed with 5 mL of a solution containing 100 mg (0.65 mmol) of 4-mercaptobenzoic acid and 0.05 g (0.21 mmol) of sodium sulfide nonahydrate in the same solvent mixture. The reaction mixture was stirred in subdued light and a nitrogen atmosphere for 12 h and yielded a yellow/white precipitate. The precipitate was isolated using conventional centrifugation and washed repeatedly using sonication/centrifugation cycles in water, methanol, and diethyl ether. The solid was dried in an evacuated drying pistol for 12 h at 80 °C over KOH. Yield 0.10 g. ^{1}H NMR (DMSO-d_6) δ (ppm): 7.0−8.0 (m, 4H arom), 12.5 (br s, acid H). FT-IR (KBr) ν (cm^{-1}): 3043 (w, arom C−H str), 2821 (w, acid OH str), 1686(s, C═O acid), 1586 (s), 1486 (s, C═C), 1395 (s, C−O−H bend), 1315 (s, C−O str), 1174 (w), 1080 (s), 1008 (m, ϕ-S), 917 (w, out-of-plane O−H bend), 813 (m,ϕ-C−H out-of-plane bend), 755 (m), 684 (w), 546(m), 521-(m), 475(m). UV−vis λ_{max} (DMF) (nm): 320 (edge), 397 (shldr).

*Mixed Surface 50% NO_2/50% CH_3 CdS Nanoclusters (**3i**).* A 50% NO_2/50% CH_3-mixed surface nanocluster was prepared as follows. Two solutions were prepared in 75 mL of a 1:1:2 CH_3OH:CH_3CN:H_2O (v:v:v) solvent system. One solution, containing 2.30 g (10 mmol) of cadmium acetate, was rapidly mixed with the other, containing 1.32 g (6.1 mmol) of $Na_2S\cdot 9H_2O$, 3.01 g (19 mmol) of 4-nitrothiophenol, and 2.43 g (20 mmol) of mercaptotoluene, yielding an orange precipitate. The reaction mixture was stirred for 12 h, after which time the solid was recovered by centrifugation. The solid was washed repeatedly by successive sonication/centrifugation cycles in, sequentially, water, acetone, methanol, and finally diethyl ether and then dried in vacuo at 65 °C in a drying pistol over KOH for 12 h. Yield: 1.23 g. The percent ratio of NO_2:CH_3 surface groups was confirmed by ^{1}H NMR integration ratios. ^{1}H NMR (DMSO-d_6) δ (ppm) 6.6−7.7 (br m, 8H, arom), 2.14 (br m, 3H, $-CH_3$). FT-IR (KBr) ν (cm^{-1}): 3016 (w, arom C−H), 2917, 2864 (w, aliph C−H), 1903, 1764 (vw, 1,4-disub ϕ ovrtn), 1613 (m), 1572 (s), 1512 (vs, NO_2 assym str), 1487 (s, ring C═C), 1337 (vs, NO_2 sym str), 1086 (s), 1012 (m, ϕ-S), 851 (m), 801(m), 741 (m), 489 (m). UV−vis (DMF) λ_{max} (nm): 404, 502.

Disulfide Syntheses. 4,4′-Dicyanophenyl disulfide, 4,4′-dicarboxydiphenyl disulfide, 4-methyl-4′-nitrophenyl disulfide, 4,4′-dihydroxyphenyl disulfide, 4,4′-dichlorophenyl disulfide, and 4,4′-dinitrophenyl disulfide were prepared using a modification of the method of Fristad et al.[6] In brief, equimolar quantities (24 mmol) of the constituent thiols were dissolved in 10 mL of DMSO and stirred for 12 h at room temperature, and the DMSO was removed in vacuo. The residues were recrystallized from acetone in the case of 4,4′-dinitrophenyl disulfide and 4,4′-dichlorophenyl disulfide, and absolute ethanol in the case of 4,4′-dimethylphenyl disulfide, 4,4′-dicyanophenyl disulfide, and 4,4′-dicarboxydiphenyl disulfide. For the mixed disulfide, an orange oil was obtained and purified by reprecipitation from acetone twice to yield a yellow oil which was used without further purification. 4,4′-Dicyanophenyl disulfide: mp 167−167.5 °C. ^{1}H NMR (DMSO-d_6) δ (ppm): 7.85 (d, 4H, C3−H), 7.71 (d, 4H, C2−H). 4,4′-Dicarboxydiphenyl disulfide: mp 310 °C (d). ^{1}H NMR (DMSO-d_6) δ (ppm): 7.93 (d, 4H, C3−H), 7.64 (d, 4H, C2−H). 4,4′-Dimethylphenyl disulfide: mp 56−59 °C (lit. 58 °C). ^{1}H NMR (DMSO-d_6) δ (ppm): 7.4 (d, 4H, C3−H), 7.12 (d, 4H, C2−H), 2.35 (s, 6H, $-CH_3$). 4,4′-Dinitrophenyl disulfide: mp 181−183 °C (lit. 182 °C). ^{1}H NMR (DMF-d_7) δ (ppm): 8.32 (d, 4H, C3−H), 7.9 (d, 4H, C2−H). 4,4′-Dichlorophenyl disulfide: mp 65−69 °C (lit. 67.5−69.5 °C). ^{1}H NMR (DMSO-d_6) δ (ppm): 7.25 (d, 4H, C3−H), 6.94 (d, 4H, C2−H). 4-Methyl-4′-nitrophenyl disulfide. ^{1}H NMR (DMSO-d_6) δ (ppm); 8.16 (d, 2H, C3′−H), 7.73 (d, 2H, C2′−H), 7.41 (d, 2H, C3−H), 7.13 (d, 2H, C2−H), 2.07 (s, 3H, $-CH_3$).

Spectroscopy. Infrared spectra were recorded as KBr pellets with a Mattson 3000 Fourier transform infrared spectrometer. ^{1}H NMR spectra were performed on a Bruker ARX 400 MHz Fourier transform nuclear magnetic resonance spectrometer in various deuterated solvents. Electronic spectroscopy was performed in 1 cm quartz cuvettes using a Hewlett-Packard 8452 diode array spectrophotometer. Fluorescence measurements were carried out on a Shimadzu RF-551 spectrofluorometric detector driven by PC-551 software with an excitation wavelength of 350 nm. Detector and monochromator systems were corrected for a differential spectral response using a $Ru(bpy)_3Cl_2$ standard. All solutions prepared for fluorescence measurements were thoroughly degassed with argon immediately prior to use. Mass spectrometry measurements were carried out using a Kratos profile mass spectrometer in EI mode at 70 eV and 2000 resolution.

Electron Microscopy. Transmission electron microscopy (TEM) was performed using a Philips EM-301 transmission electron microscope. Nanocluster samples were prepared by placing a few drops of a freshly sonicated and centrifuged DMF suspension of the desired cluster (2.5 mg of nanocluster in 3 mL of solvent) onto J. B. EM Sevices (Point Claire, Dorval, Quebec) JBS-183 300 mesh carbon-coated copper grids (cleaned in acetone and chloroform, and again in acetone followed by air-drying). The excess solvent was drawn off with a piece of filter paper while holding the grid in noncapillary forceps, leaving aggregates as well as individual nanoclusters adhering to the surface. Grids were then air-dried at room temperature. Size calibration was performed using a precision silicon grid of 21600 lines cm^{-1}.

Table 1. HPLC Solvent Profile Used for the Separation of Photolysis Product Mixtures of 3a−k

time (min)	% methanol
0	50
8	90
11	90
12	90
16	90
18	90

Photochemical Irradiation. All sample preparations were carried out in subdued light with the aid of a Kodak 1A safelight. Fifty milligrams of the desired cluster was suspended in 50 mL of DMF with sonication, and the suspension was carefully centrifuged. The supernatant was divided into five 8 mL aliquots placed in quartz vials. The remaining solution was stored in total darkness. Suspensions were thoroughly degassed with argon and exposed to the illumination (maximum 350 nm) of a 175 W high-pressure mercury vapor lamp (Philips H39KB-175, UV shield removed) under an atmosphere of argon while the temperature was maintained at 27 ± 2 °C. Samples were removed to darkness at sequential 20 min intervals over a period totaling 100 min. The yellow precipitate which formed in each vial was separated out by centrifugation upon removal from the UV chamber, and the supernatant was immediately analyzed by HPLC.

High Performance Liquid Chromatography (HPLC). Samples were prepared by transferring 2000 μL of the irradiated suspension and 250 μL of benzene to a darkened scintillation vial using a precision autopipet (Eppendorf). All separations were carried out using a Hewlett-Packard 1050 Series liquid chromatography system fitted with a fixed wavelength (350 nm) UV detector and 40 μL injection loop. The stationary phase was Supelcosil LC-8 5 μm functionalized silica packed in a 25.0 cm long, 4.6 mm diameter column (Supelco no. 017974AB). The eluent for these separations was a mixture of water and methanol in varying relative percentages, as outlined in Table 1. Separations were conducted at 1 mL/min.

Results and Discussion

The covalent attachment of luminescent, electroactive, or electrooptic molecular species to the surfaces of functionalized semiconductor nanoclusters will undoubtedly become a major strategy in the fabrication of new and unusual quantum dot-based electronic devices. Thus, we[6] and others[8] have been investigating the synthesis and reactivity of surface-functionalized semiconductor nanoclusters. However, the degree to which a remote surface substituent interacts electronically with the nanocluster core remains an important question. During the course of our studies concerning surface-substituted ∼30 Å thiolate-capped CdS nanoclusters, we observed that systems baring an aniline surface undergo steady decomposition upon exposure to room lighting, while the same nanoclusters for which the amino groups had been amidized do not appreciably

(7) Fristad, W. E.; Peterson, J. R. *Synth. Commun.* **1985**, *15*, 1.

(8) (a) Torimoto, T.; Maeda, K.; Maenaka, J.; Yoneyama, H. *J. Phys. Chem.* **1994**, *98*, 13658. (b) Nosaka, Y.; Ohta, N.; Fukuyama, T.; Fujii, N. *J. Colloid Interface Sci.* **1993**, *155*, 23. (c) Torimoto, T.; Uchida, H.; Sakata, T.; Mori, H.; Yoneyama, H. *J. Am. Chem. Soc.* **1993**, *115*, 1874. (d) Stipkala, J. M.; Castellano, F. N.; Heimer, T. A.; Kelly, C. A.; Livi, K. J. T.; Meyer, G. J. *Chem. Mater.* **1997**, *9*, 2341. (e) Gacoin, T.; Malier, L.; Boilot, J.-P. *Chem. Mater.* **1997**, *9*, 1502. (f) Løver, T.; Henderson, W.; Bowmaker, G. A.; Seakins, J. M.; Cooney, R. P. *Chem. Mater.* **1997**, *9*, 1878.

decompose under room illumination, even after prolonged exposure to the lights. As the rate of decomposition appears to be controlled by the nature of a remote substituent on the capping agent, the photodecomposition mechanism likely involves facile electronic communication between the semiconductor core and the organic surface. Hence, we undertook a study of the photodecomposition kinetics of a variety of surface-substituted thiolate-capped CdS nanoclusters. Substituents were introduced onto the surface of ~30 Å CdS nanoclusters as previously described. Chemical and physical properties of substituted thiolate-capped CdS nanoclusters, as well as full characterization methods and polydispersities, have been discussed earlier.[3−5] Eight substituted nanoclusters, **3a**−**h**, were prepared by the kinetic trapping method outlined in eq 1. Two

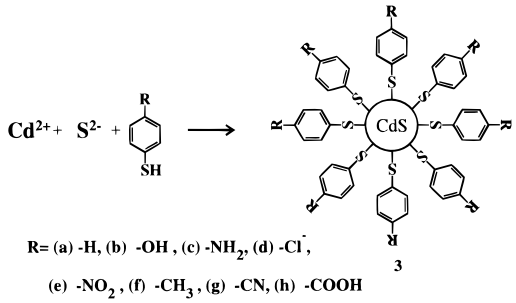

other nanoclusters, the acetamide, **3k**, and acetyl surface systems, **3j**, were obtained by derivatization of $QDNH_2$, **3c**, and QDOH, **3b**, repsectively, as previously described (eq 2 and 3).[6c,d] All preparative and subse-

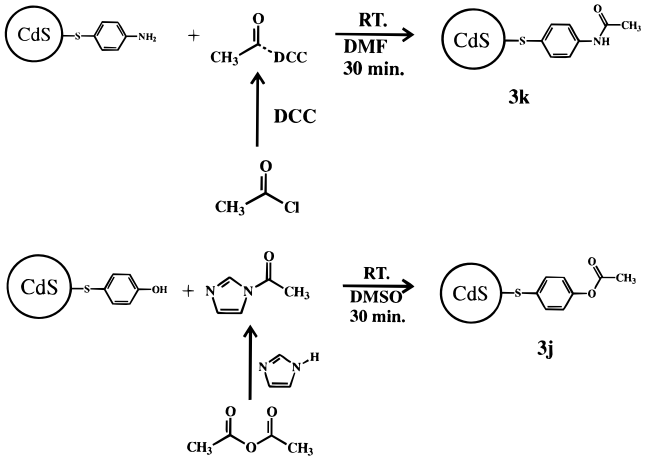

quent procedures were performed in inert atmosphere and under the subdued illumination of a photographic safelight. Cluster diameters were estimated by electronic spectroscopy (Figure 5), in accordance with a tight-binding band analysis,[9] and cluster diameters and size distributions were determined more directly by transmission electron microscopy (Table 2) and are in good agreement with X-ray analysis as described earlier.[6,9a] Six 8 mL samples of each nanocluster were prepared in DMF. One sample was stored in total darkness and acted as a control, while the other five were exposed for 20, 40, 60, 80, and 100 min, respectively, to the emission of a high-pressure mercury vapor lamp. Each illuminated sample became opalescent, and in some a yellow precipitate began to settle out. This

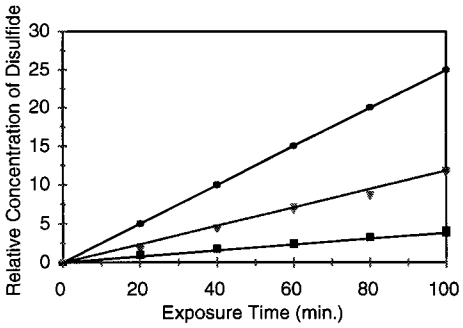

Figure 1. Rate of formation of symmetric disulfides from the photolysis of **3a** (■- - -■); **c** (▼- - -▼), **g** (●- - -●).

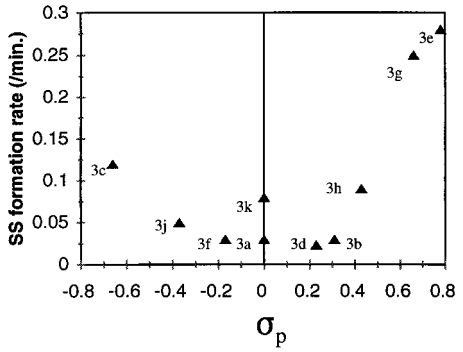

Figure 2. Correlation between disulfide formation rate and surface substituent Hammett parameter, σ_p, for nanoclusters **3a**−**h**, **3j**, and **3k**.

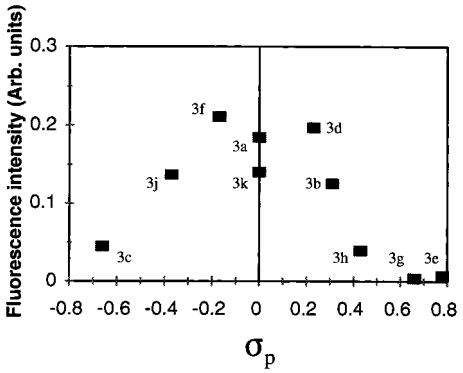

Figure 3. Dependence of excitonic fluorescence intensity of nanoclusters **3a**−**h**, **3j**, and **3k** on surface substituent Hammett parameter σ_p.

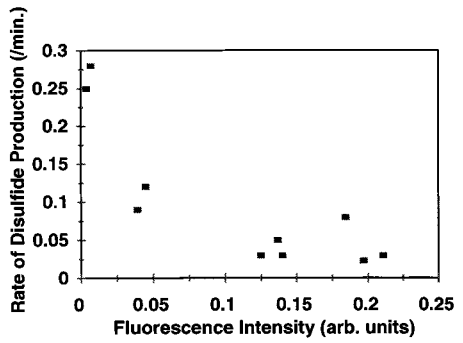

Figure 4. Correlation between disulfide photoproduction rate and excitonic fluorescence intensity in nanoclusters **3a**−**h**, **3j**, and **3k**.

(9) (a) Wang, Y.; Herron, N. *Phys. Rev. B* **1990**, *42*, 7253. (b) Wang, Y.; Herron, N. *J. Phys. Chem.* **1991**, *95*, 525. (c) Vossmeyer, T.; Katsikas, L.; Giersig, M.; Popovic, I. G.; Diesner, K.; Chemsddine, A.; Eychmüller, A.; Weller, H. *J. Phys. Chem.* **1994**, *98*, 7665.

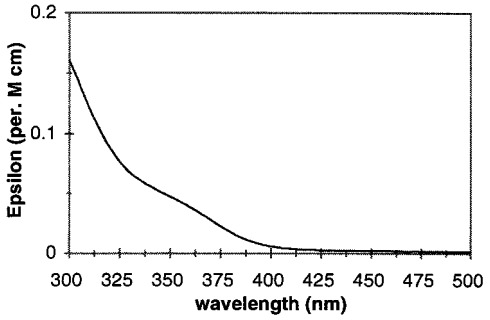

Figure 5. Electronic spectrum of a DMF suspension of **3f** showing the characteristic excitionic shoulder at 390 nm.

Table 2. Diameters of 3a-k as Determined Using TEM and Electronic Spectroscopy

cluster	λ (nm)[a]	TEM diameter (Å)[c]	calculated diameter (Å)[d,e]
3a	380	33 ± 7	24
3b	390	30 ± 7	24
3c	360	27 ± 8	22
3d	360	29 ± 7	22
3e	324, 400,[b] 502	30 ± 7	
3f	390	31 ± 7	24
3g	395	26 ± 7	24
3h	397	27 ± 7	24
3i	404,[b] 502	30 ± 7	
3j	380	28 ± 7	25
3k	390	24 ± 7	24

[a] CdS band-to-band absorption unless otherwise noted. [b] n-π^* absorption of NO_2. [c] Transmission electron microscopy. 7 Å represents the resolution limit of the microscope. [d] Tight-binding band theory. [e] Tight-binding band theory deviates as much as 20% from experimental X-ray analysis for similarly prepared CdS nanoclusters in the size regime of 20 Å; please refer to ref 9a for detailed discussion.

precipitate was found to be insoluble in CS_2, confirming that colloidal sulfur was not produced during the photolysis procedure. No precipitate or opalescence was observed in the control sample for any of the substituted nanoclusters. Following centrifugation to remove any precipitated solid, each sample (including the control) was mixed with a benzene standard and subjected to HPLC analysis. In all cases one single product (in addition to the yellow precipitate) was found, and unambiguously identified (by ^{1}H NMR analysis and HPLC standard addition methods) as the corresponding symmetric disulfide, the concentration of which was monitored relative to the internal benzene standard. Only trace amounts of disulfide could be detected in any of the control samples. Authentic samples of each disulfide were synthesized and injected into the HPLC to confirm the retention times relative to the benzene standard. The authentic disulfides were also used to determine sensitivity factors so that the concentrations of disulfide in the photodecomposed supernatants can be quantified.

The rate of disulfide generation as a function of exposure time for a selected series of nanoclusters studied is presented in Figure 1. A summary of decomposition data and approximate optical density data for **3a**−**h**, **3j**, and **3k** may be found in Table 3. The estimated optical densities presented rely on two fundamental assumptions; first, that colloidal suspensions obey Beer's law, and the second, that the density of bulk CdS is a suitable estimate of the density of the cluster core and thus its molecular weight. It is thus somewhat surprising that such good agreement between the optical densities of the different clusters at the irradiation and excitation wavelength is observed.

Table 3. Summary of Photodecomposition Data for 3a−h, 3j, and 3k

compound	photolysis rate (min^{-1})	R^2	optical density[a] at 350 nm (M^{-1} cm^{-1})
3a	0.03	0.987	0.108
3b	0.04	0.992	0.113
3c	0.12	0.992	0.082
3d	0.023	0.987	0.063
3e	0.28	0.992	0.262
3f	0.03	0.980	0.082
3g	0.25	0.999	0.072
3h	0.09	0.999	0.076
3i			0.191
3j	0.03	0.992	0.090
3k	0.08	0.984	0.070

[a] Optical density was approximated for nanocluster suspensions using the molecular weight of a cluster determined using TEM radius data and the density of bulk CdS (4.8 g mL^{-1}).

In all cases the photodecomposition proceeds at a constant rate. The ring substituent, para to the point of attachment to the nanocluster, affects the rate of disulfide photoproduction in an interesting way. Both strongly electron-donating and strongly electron-accepting substituents enhance the photodecomposition rate relative to the unsubstitued thiolate, while *p*-chloro somewhat stabilizes the nanocluster. Amidization reduces the decomposition rate of the aniline surface quantum dot significantly, presumably because of the delocalization of the nitrogen lone pair to the carbonyl oxygen. The photodecomposition rate of the substituted nanoclusters plotted against the corresponding Hammett σ_p substituent parameter is presented in Figure 2, and confirms the general trend that the photodecomposition is enhanced by both electron donors and acceptors.

Interestingly, the relationship between the photodecomposition rate and the Hammett parameter of the substituent on the attached thiolate appears to be mirrored by the fluorescence data of the substituted quantum dots; both strongly electron-donating and strongly electron-accepting substituents very effectively quench the nanocluster fluorescence, while *p*-chloro and methyl slightly enhance the fluorescence relative to the unsubstituted species. Integrated fluorescence intensities of the substituted nanoclusters as a function of the Hammett σ_p parameter appear in Figure 3. Figures 2 and 3 suggest a definite relationship between the rate of photodecomposition and the luminescence quenching efficiency of the remote substituent. This relationship is presented graphically in Figure 4 and indicates that destruction of the CdS exciton by surface-induced hole or electron capture is involved in the photodecomposition mechanism. For a strongly electron-donating surface, the band edges in the nanocluster core bend upward in energy as they approach the surface, as illustrated in Figure 6. Likewise, in the case of a strongly electron-withdrawing surface, the surface will possess a greater effective electronegativity than the core and the band edges will consequently bend downward (Figure 6). In the former case, a photogenerated exciton will separate, as the electron sinks down the conduction band into the interior of the quantum dot while the hole floats up the valence band toward the surface. In the latter situation, the exciton will again separate, with

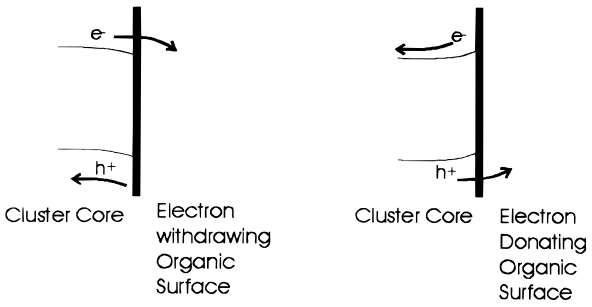

Figure 6. Surface substituent induced band-bending in substituted thiolate-capped CdS semiconductor nanoclusters.

Scheme 1

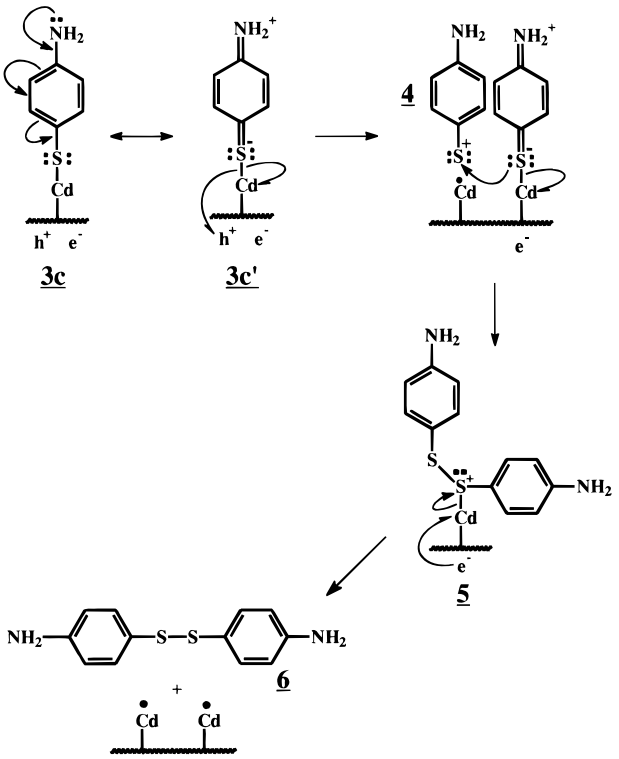

the hole floating toward the core while the electron sinks to the surface (see Figure 6). In either case, exciton separation results in fluorescence quenching. For intermediate cases, where the bands are relatively flat, fluorescence is observed to varying degrees.

Once at the surface, photogenerated holes or electrons can act as relatively energetic oxidizing or reducing species, respectively, where they can be captured by the surface capping groups. The mechanism in the case of an electron-donating surface ($QDNH_2$) is illustrated in Scheme 1. Delocalization of the amine lone pair can be represented by the canonical resonance form **3c′**, rendering the thiolate sulfur atom relatively electron-rich. The photogenerated hole captures an electron from the Cd−Sϕ σ-bond, producing a highly electrophilic phenylsulfenium ion, **4**, and a dangling bond on the quantum dot. The phenylsulfenium ion electrophilically attacks a sulfur lone pair on a neighboring thiolate, yielding the cadmium-bound intermediate ion, **5**, which eventually captures the remaining electron, producing another dangling surface bond and the product disulfide, **6**. As the concentration of surface-dangling bonds increases, the quantum dots begin to coalesce into macroscopic

Scheme 2

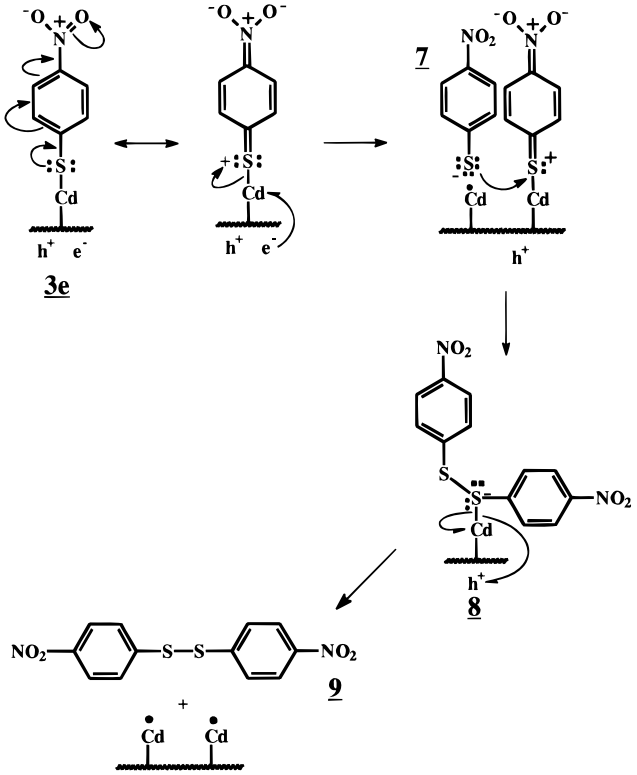

particles, rendering the solution opalescent. The photodecomposition mechanism for acceptor surface nanoclusters ($QDNO_2$) is analogous and is presented in Scheme 2. The thiolate sulfur atom is relatively electron-deficient as a result of resonance delocalization of the sulfur lone pair. Reduction by the photogenerated electron results in a phenylsulfide ion, **7**, which can nucleophilically attack the electron-deficient sulfur of a neighboring thiolate. The cadmium bound anion, **8**, eventually captures the remaining hole, again producing the free disulfide, **9**, and two dangling surface bonds. For surfaces of intermediate electron demand, the exciton recombination rate is higher than, or competitive with, the surface carrier capture rate arresting decomposition, as heralded by the CdS luminescence. Further support of the above-described mechanism was obtained from the product distribution following the photodecomposition of a 1:1 NO_2/CH_3-mixed surface nanocluster (**3i**). Random formation of disulfide would result in a 1:2:1 mole ratio of products **9:10:11**. However, what was actually observed is a mole ratio distribution of 3:1:1, in accord with our mechanism in which the anionic 4-nitrophenyl sulfide intermediate, **7**, preferentially attacks the electron-deficient sulfur of a neighboring nitrothiolate.

Conclusions

The unusual optical and electronic properties of semiconductor quantum dots distinguish them as prime candidates for the eventual fabrication of novel electronic devices. Such devices will undoubtedly involve surface activation and covalent bonding of interesting molecular moieties to the nanoclusters. Facile electronic communication between the semiconductor core and the surface functionalities is an important criterion for the

realization of device activity in these systems. We have previously shown that a wide scope of interesting molecular moieties can be covalently tethered onto the surface of CdS nanoclusters, and that the properties of the resulting systems depend to a great extent on the nature of the surface groups. In this contribution, we demonstrated that ~30 Å thiolate-capped CdS nanoclusters photodecompose to form bulk CdS and a single organic product, the symmetric disulfide corresponding to the thiolate cap, and further studied the effects of surface modification on the rate of photodecomposition. We found that the decomposition rate is enhanced by both electron donors and acceptors in the 4-position of the thiolate capping agent, and is strongly correlated with the fluorescence quenching efficiency of the substituted cap. We present a likely mechanism for the photodecomposition, implying facile electronic contact between the nanocluster core and remote substituents on the surface groups.

Acknowledgment. We are indebted to Dr. Abdiaziz Farah and Professor A. B. P. Lever and his research group for their valuable discussions and suggestions, to Karen Rethoret for assistance with the electron microscopy, to Lisa Nelson for assistance with mass spectroscopy, and to Professor Rob McLaren and Carolyn Hempstead for assistance with the HPLC equipment. We also acknowledge the Natural Sciences and Engineering Research Council of Canada (NSERC) for their generous financial support.

CM980513T